analytical chemistry

Technical Note

pubs.acs.org/ac

Influx and Production Rates in Peak-Mode Isotachophoresis

Charbel Eid and Juan G. Santiago*

Department of Mechanical Engineering, Stanford University, Stanford, California 94305, United States

Supporting Information

ABSTRACT: We present an analytical model useful in the design of peak-mode isotachophoresis (ITP) experiments. The model quantifies sample influx and production rates, the latter in applications where ITP is used to accelerate chemical reactions. We include analysis of the effect of initial sample placement location. We derive and identify key nondimensional parameters for the general case of weak electrolyte buffer ions in terms of sample placement (injection mode), initial concentrations, fully ionized mobilities, and reaction kinetic constants. We then discuss how to use these parameters in the optimal design of peak-mode ITP assays and highlight regimes of particular interest. We clearly identify a quasi-equilibrium regime wherein production rates increase until they equal the influx rate of the low abundance sample species. The model and analysis are generally applicable to both cationic and anionic ITP assays and likely to a wide range of sample species.

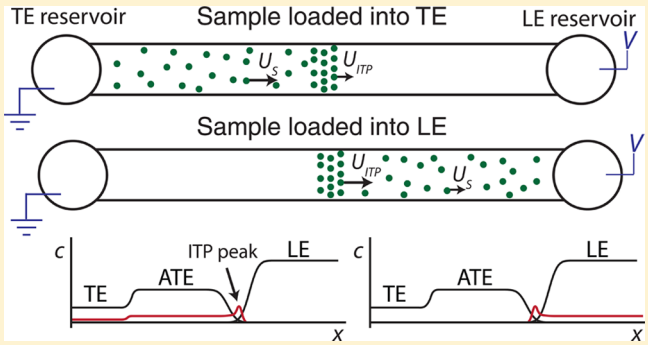

Isotachophoresis (ITP) is a well-established electrophoretic separation and preconcentration technique used in a wide range of chemical and biomedical applications.[1−3] ITP uses a heterogeneous two-buffer system consisting of a high-mobility leading electrolyte (LE) buffer and a low-mobility trailing electrolyte (TE) buffer. Sample ions with effective mobilities greater than those of the TE (co-ion) in the TE buffer and less than those of the LE (co-ion) in the LE buffer focus at an interface between the TE and LE. When sample species are present in sufficiently high concentrations, they segregate into adjacent but distinct zones, called plateaus, with locally uniform concentrations. However, at low concentrations, sample ions cofocus into one or more partially overlapping sharp peaks. This "peak-mode" ITP is particularly relevant in biological applications, where species such as nucleic acids and proteins are often found in concentrations several orders of magnitude below those of the LE and TE.

Peak-mode ITP has been extensively used in sample preparation and applied to the extraction of nucleic acids and/or proteins from blood,[4−7] serum,[8−11] urine,[12,13] milk,[14] and other complex samples. ITP has also been used to accelerate reactions and substantially reduce assay times, by over 10 000-fold.[15]

Effective design of peak-mode ITP assays requires consideration of several coupled phenomena. Several studies have analyzed focusing dynamics,[16−18] sample distribution,[19,20] and dispersive forces[18,19,21,22] influencing sample preconcentration. Rogacs et al.[7] recently discussed various design choices and parameters in the context of ITP nucleic acid purification. Several studies analyzed ITP assays for reaction acceleration and separation. Bercovici et al.[15] developed a reaction model for ITP-aided hybridization assays wherein two reactants are focused in ITP, while Eid et al.[23] explored the design of assays in which a spacer molecule is used to separate reactants and products. Karsenty et al.,[24] Han et al.,[25] and Shkolnikov et al.[26] analyzed ITP assays between a stationary probe and a focused nucleic acid species. Recently, Rubin et al.[20] presented a significant extension of the model by Bercovici et al.,[15] incorporating peak shapes and production rates for the case of purely diffusive dispersion and asymmetric ITP peaks that partially overlap. Despite these studies, we know of no simple-to-use engineering models that identify key figures of merit and can be applied to optimize ITP influx and production rates as a function of sample properties and various injection strategies (i.e., initial placement) of samples.

In Figure 1, we depict two loading configurations which we consider here. Sample ions with intermediate mobilities can be mixed initially with either TE or LE buffers and will focus in ITP. However, the rate at which sample ions enter the ITP zone can vary significantly. This rate depends on mobilities of the different ionic species, buffer concentrations and compositions, and channel and chip geometry.

We here present an analytical model that describes the effect of initial sample placement on influx and production rates (reaction rates) in ITP. We concentrate on the case of negligible bulk flow and wherein sample is injected into a channel section prior to initiation of ITP. However, our analyses are extendable to other configurations, such as when sample is injected from a TE sample reservoir (we analyze this case in the Supporting Information). We do not consider cases

Received: September 2, 2016
Accepted: October 21, 2016

DOI: 10.1021/acs.analchem.6b03467
Anal. Chem. XXXX, XXX, XXX−XXX

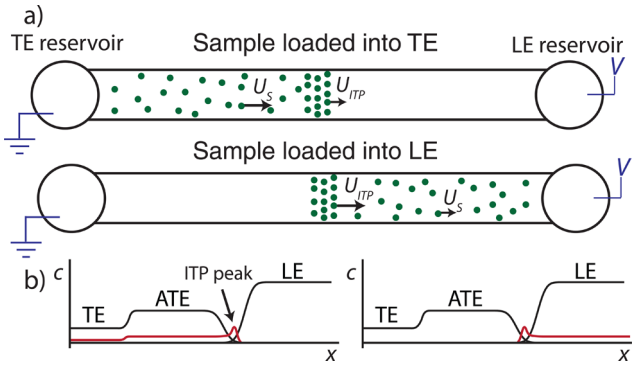

Figure 1. (a) Schematic representation of an ITP assay showing two loading configurations. In the first, sample is loaded in the TE zone and overspeeds TE co-ions to focus at the ITP peak. In the second, sample is loaded in the LE and is oversped by the LE co-ions. (b) Plots of species concentrations in the different zones. We greatly exaggerated sample zone concentrations (red curve) versus typical initial values for clarity of presentation.

in which sample is loaded into both LE and TE (e.g., at the same concentration). The latter case is guaranteed to yield maximal influx and production rates but is the least convenient experimentally and the least interesting analytically.

We begin with a simple formulation for sample concentration in the adjusted TE (ATE) zone. The ATE zone is the zone formed by TE ions as they migrate into a region formerly occupied by the LE.[3] We then define a dimensionless parameter that relates the rate of sample influx in ITP to initial sample placement. Finally, we discuss the effect of initial sample placement on ITP-aided reaction assays.

THEORY

In addition to the simplifications discussed above, we also here assume net charge neutrality in all zones.[27] In neglecting bulk flow, we also neglect advective currents. We will express ionic current in regions well away from the ITP interfaces (within TE, ATE, or LE plateaus), so we assume diffusive currents are negligible.[15] Further, we assume that the charge relaxation time scale is negligibly small, so we can obtain relations for electric fields in terms of conservations of ionic current.[27] We assume sample ions focusing in peak-mode ITP at constant current have negligible contribution to local conductivity due to their low concentration.[18]

Sample Concentration in the Adjusted TE. Under our assumptions, the composition of the adjusted TE zone can be obtained using Jovin[28] and Alberty's[29] relations and is given by[18,30]

$$c_{\mathrm{TE}}^{\mathrm{ATE}} = \frac{\mu_{\mathrm{TE}}^{0}}{\mu_{\mathrm{LE}}^{0}}\left(\frac{\mu_{\mathrm{CI}}^{0}-\mu_{\mathrm{LE}}^{0}}{\mu_{\mathrm{CI}}^{0}-\mu_{\mathrm{TE}}^{0}}\right)c_{\mathrm{LE}} \tag{1}$$

Here, μ^0 is the (fully ionized) electrophoretic mobility, defined as the ratio of velocity and electric field. Superscripts refer to zones and subscripts identify the ion of interest. The subscripts LE, TE, and CI refer, respectively, to LE, TE, and the counterion. We assume that the fully ionized mobilities of LE, TE, and sample ions are constant and independent of zone (e.g., $\mu_{\mathrm{s}}^{\mathrm{LE},0} \approx \mu_{\mathrm{s}}^{\mathrm{TE},0} \approx \mu_{\mathrm{s}}^{0}$), so we neglect ionic strength effects.[31] In the Supporting Information, we offer a more detailed derivation of eq 1, as well as a discussion of effective and fully ionized buffer and sample mobilities. We define β as the ratio of TE ion concentrations in the ATE and TE zones:

$$\beta \equiv \frac{c_{\mathrm{TE}}^{\mathrm{ATE}}}{c_{\mathrm{TE}}^{\mathrm{TE}}} = \frac{\mu_{\mathrm{TE}}^{0}}{\mu_{\mathrm{LE}}^{0}}\left(\frac{\mu_{\mathrm{CI}}^{0}-\mu_{\mathrm{LE}}^{0}}{\mu_{\mathrm{CI}}^{0}-\mu_{\mathrm{TE}}^{0}}\right)\frac{c_{\mathrm{LE}}}{c_{\mathrm{TE}}^{\mathrm{TE}}} \tag{2}$$

We see that β is directly proportional to the ratio of initial LE and TE concentrations. This ratio is an important, controllable parameter in the design of ITP assays.[18] We thus define

$$\gamma = \frac{c_{\mathrm{LE}}}{c_{\mathrm{TE}}^{\mathrm{TE}}} \tag{3}$$

Combining eqs 1 and 2 along with mass conservation, we express the concentration of sample ions in the ATE zone as

$$c_{\mathrm{s}}^{\mathrm{ATE}}E^{\mathrm{ATE}} = c_{\mathrm{s}}^{\mathrm{TE}}E^{\mathrm{TE}} \tag{4}$$

$$c_{\mathrm{s}}^{\mathrm{ATE}} = c_{\mathrm{s}}^{\mathrm{TE}}\left(\frac{E^{\mathrm{TE}}}{E^{\mathrm{ATE}}}\right) = c_{\mathrm{s}}^{\mathrm{TE}}\left(\frac{\sigma^{\mathrm{ATE}}}{\sigma^{\mathrm{TE}}}\right) = c_{\mathrm{s}}^{\mathrm{TE}}\left(\frac{c_{\mathrm{TE}}^{\mathrm{ATE}}}{c_{\mathrm{TE}}^{\mathrm{TE}}}\right) = \beta c_{\mathrm{s}}^{\mathrm{TE}} \tag{5}$$

This relation is useful when sample is initially loaded into the TE zone.

Sample Ion Influx Rate in ITP. For sample ions initially loaded into (mixed with) the TE, their rate of influx into the ITP zone is given by

$$Q_{\mathrm{s}}^{\mathrm{ATE}} = (U_{\mathrm{s}}^{\mathrm{ATE}} - U_{\mathrm{ITP}})Ac_{\mathrm{s}}^{\mathrm{ATE}} = \left(\frac{\mu_{\mathrm{s}}^{0}}{\mu_{\mathrm{TE}}^{0}} - 1\right)U_{\mathrm{ITP}}Ac_{\mathrm{s}}^{\mathrm{ATE}} \tag{6}$$

where $U_{\mathrm{s}}^{\mathrm{ATE}}$ is the velocity of sample in the ATE zone, U_{ITP} is the velocity, and A is the cross-sectional area. Q is derived through a control volume analysis around the ITP interface. This flux is proportional to the relative velocities of the sample and TE ions. For sample ions initially loaded into the LE, influx rate into the ITP zone is given by

$$Q_{\mathrm{s}}^{\mathrm{LE}} = (U_{\mathrm{ITP}} - U_{\mathrm{s}}^{\mathrm{LE}})Ac_{\mathrm{s}}^{\mathrm{LE}} = \left(1 - \frac{\mu_{\mathrm{s}}^{0}}{\mu_{\mathrm{LE}}^{0}}\right)U_{\mathrm{ITP}}Ac_{\mathrm{s}}^{0} \tag{7}$$

We define so-called separabilities, first introduced by Bocek[32] and then further explored by Marshall[33]

$$p_{\mathrm{s,TE}} = \frac{\mu_{\mathrm{s}}^{0}}{\mu_{\mathrm{TE}}^{0}} - 1, \qquad p_{\mathrm{s,LE}} = 1 - \frac{\mu_{\mathrm{s}}^{0}}{\mu_{\mathrm{LE}}^{0}} \tag{8}$$

Separability quantifies the relative mobilities of the sample ion and surrounding TE or LE ions. So we recast eqs 6 and 7 as

$$Q_{\mathrm{s}}^{\mathrm{ATE}} = (U_{\mathrm{s}}^{\mathrm{TE}} - U_{\mathrm{ITP}})Ac_{\mathrm{s}}^{\mathrm{ATE}} = p_{\mathrm{s,TE}}U_{\mathrm{ITP}}A\beta c_{\mathrm{s}}^{0} \tag{9}$$

and

$$Q_{\mathrm{s}}^{\mathrm{LE}} = (U_{\mathrm{ITP}} - U_{\mathrm{s}}^{\mathrm{LE}})Ac_{\mathrm{s}}^{\mathrm{LE}} = p_{\mathrm{s,LE}}U_{\mathrm{ITP}}Ac_{\mathrm{s}}^{0} \tag{10}$$

where c_{s}^{0} is the initial sample concentration loaded into either TE or LE, respectively. In the Supporting Information, we present derivations for influx rate for the case of partially ionized TE co-ions and fully ionized sample ions. The ratio of

DOI: 10.1021/acs.analchem.6b03467
Anal. Chem. XXXX, XXX, XXX−XXX

these two (steady) molar fluxes guides optimal initial sample placement; hence, we define

$$\phi \equiv \frac{Q_s^{ATE}}{Q_s^{LE}} = \frac{p_{s,TE}}{p_{s,LE}}\beta \tag{11}$$

Unity is a threshold value for ϕ. For $\phi > 1$, sample ions should be loaded in the TE. For $\phi < 1$, they should be loaded into the LE. Alternatively, we can define a threshold sample mobility:

$$\mu_s^{thres} = \frac{(1+\beta)\mu_{TE}^0\mu_{LE}^0}{\beta\mu_{LE}^0 + \mu_{TE}^0} \tag{12}$$

Sample ions with mobility greater than μ_s^{thres} should be placed in TE; those with lower mobility should be placed into LE zone.

Production Rate in ITP-Aided Reaction Assays. ITP can be used to accelerate reactions, when one or more sample species is focused in ITP. We here consider a second-order chemical reaction between two ionic reactants A and B, A + B ⇄ AB, where both are focused by ITP (e.g., RNA and cDNA in anionic ITP[15,34]), although our approach can be extended to other cases. We limit our analysis to the domain wherein production rates are significantly greater in the ITP zone than in the LE or TE zones. This assumption largely holds when both reactant species are focused and preconcentrated in ITP, but this should be reconsidered when only a single species is focused in ITP (Eid et al.[11] describes a two-region reaction model for such a case). Bercovici et al.[15] first developed a mass-action reaction model incorporating ITP preconcentration. They made the simplifying assumption that ITP zones had a Gaussian profile and were perfectly overlapped and then used volume-averaged concentrations of that profile. Garcia et al.[19] first showed that ITP peaks may exhibit very asymmetric, non-Gaussian profiles, and derived approximate analytic expressions for both purely diffusive and dispersive (Taylor type dispersion) profiles. As we mentioned earlier, Rubin et al.[20] presented closed-form solutions for peak shapes and production rates for the case of pure diffusion and electromigration. Their model takes into account asymmetric ITP peaks with partial overlap. This nonideal behavior has the effect of lowering production rates. We here apply Rubin's model to analyze initial sample placement. The governing equations for Rubin's model are volume averages of conservation of species equations as follows:

$$\begin{cases} \dfrac{dN_A^j}{dt} = Q_A^j - k_{on}^{eff}N_AN_B + k_{off}N_{AB} \\ \dfrac{dN_B^j}{dt} = Q_B^j - k_{on}^{eff}N_AN_B + k_{off}N_{AB} \\ \dfrac{dN_{AB}^j}{dt} = k_{on}^{eff}N_AN_B - k_{off}N_{AB} \end{cases} \tag{13}$$

The superscript j represents LE or ATE, depending on the location of the reactant during ITP. N_A, N_B, and N_{AB} represent the number of moles of A, B, and the hybrid AB, respectively. Here, k_{on}^{eff} and k_{off} denote the effective association and dissociation rate constants, respectively. Rubin et al.[20] found that production rates depend significantly on sample distribution within the ITP zone. The term k_{on}^{eff} results from the fact that the ITP-focused peaks of A and B are not perfectly Gaussian and do not perfectly aligned is defined as follows

$$k_{on}^{eff} = k_{on}k_{form} \tag{14}$$

where k_{on} is the standard association rate constant, and k_{form} is a dimensional (units over inverse volume) mobility-dependent correction factor, given by

$$k_{form} = \frac{1}{\pi A\delta}\frac{1-(y_A+y_B)}{\cot(\pi y_A)+\cot(\pi y_B)} \tag{15}$$

and

$$y_A = \frac{1/\mu_{TE}^0 - 1/\mu_A^0}{1/\mu_{TE}^0 - 1/\mu_{LE}^0},\ y_B = \frac{1/\mu_{TE}^0 - 1/\mu_B^0}{1/\mu_{TE}^0 - 1/\mu_{LE}^0} \tag{16}$$

Rubin et al.[20] found that for symmetric peaks, k_{form} is maximized when reactants are maximally overlapped (i.e., $y_A = y_B = 0.5$). However, when reactants have asymmetrical concentration profiles, k_{form} is not necessarily maximized when the peak concentration regions strongly overlap. For each of the two reacting species, and neglecting reactant depletion, the total species amount at any time is related to the influx rate of that species in ITP, such that

$$\begin{aligned} N_A^j + N_{AB}^j &= Q_A^j t, \\ N_B^j + N_{AB}^j &= Q_B^j t \end{aligned} \tag{17}$$

For simplicity, we assume, as did Rubin et al.,[20] that one species is in excess so that

$$N_A^j \gg N_B^j \tag{18}$$

where j represents LE or ATE zone, as above. This inequality ensures that one species is in excess in ITP (we will refer to this as reactant A). Under this assumption, we can derive a form of Rubin's eq 59 for A in the LE and B in the ATE as follows:

$$\begin{aligned} N_{AB}^j(t) = {} & \frac{Q_A^jQ_B^j}{(Q_A^j+Q_B^j)^2}\frac{k_{off}}{k_{on}^{eff}}e^{-(J_1)^2} \\ & [e^{(J_2)^2}(1-(1-J_3)e^{(1-0.5J_3)k_{off}t}) + 0.5 \\ & J_2\sqrt{\pi}(1-2(J_2)^2)(\mathrm{erfi}(J_2) - \mathrm{erfi}(J_1))] \end{aligned} \tag{19}$$

where,

$$J_1 = \frac{k_{off} + ak_{on}^{eff}t}{\sqrt{2ak_{on}^{eff}}},\quad J_2 = \frac{k_{off}}{\sqrt{2ak_{on}^{eff}}},\quad J_3 = \frac{ak_{on}^{eff}t}{k_{off}} \tag{20}$$

Note the dimensionless form of eq 19 can be obtained easily by dividing by the prefactor Q_Bt, a formulation we will use below. Again following Rubin et al., we define τ as the reaction time scale for an ITP-aided reaction assay as

$$\tau^j = \frac{k_{off}}{(Q_A^j+Q_B^j)k_{on}^{eff}} \tag{21}$$

For times greatly exceeding τ, we can recast eq 19 in terms of the dimensionless production rate $\hat{N}_{AB}^j$ as

$$\hat{N}_{AB}^j(t \gg \tau) \equiv \frac{N_{AB}^j}{Q_Bt} = \frac{Q_A^j}{Q_A^j+Q_B^j} \tag{22}$$

DOI: 10.1021/acs.analchem.6b03467
Anal. Chem. XXXX, XXX, XXX−XXX

Expanding the simplification presented in eq 18 to also include the most common case where the influx rate of the abundant analyte is greater than that of low abundance, $Q_A^j \gg Q_B^j$, eq 22 simplifies to

$$\hat{N}_{AB}^{j}(t \gg \tau) \cong 1 \tag{23}$$

This result implies that, after some transience associated with kinetic rates, the production rate due to the chemical reaction will rise until it is equal to (and limited by) the net influx rate of the low-abundance species. Initial injection schemes and ITP conditions which maximize influx rate also maximize production rate. In Table 1, we summarize several important parameters that influence the optimal design of peak-mode ITP assays.

Table 1. Key Parameters Defined and Derived Which Characterize Sample Influx and Production Rate As a Function of Initial Placement of Sample in TE or LE

symbol	interpretation	definition
β	ratio of sample concentration in ATE and TE zones	$\beta = \frac{c_{TE}^{ATE}}{c_{TE}^{TE}}$
γ	ratio of initial LE and TE ion concentrations	$\gamma = \frac{c_{LE}}{c_{TE}^{TE}}$
ϕ	ratio of sample influx fluxes into ITP from TE and LE	$\phi = \frac{p_{s,TE}}{p_{s,LE}}\beta$
μ_s^{thres}	threshold sample mobility for loading in LE or TE	$\mu_s^{thres} = \frac{(1+\beta)\mu_{TE}\mu_{LE}}{\beta\mu_{LE}+\mu_{TE}}$
τ^j	reaction time scale in ITP-aided reaction	$\tau^j = \frac{k_{off}}{(Q_A^j + Q_B^j)k_{on}^{eff}}$
ε	ratio of product formation in ITP-aided reactions for reactants loaded in TE and LE	$\varepsilon = \frac{N_{AB}^{TE}}{N_{AB}^{LE}}$

Initial sample placement in an ITP-aided reaction assay is an important design parameter. We here consider the configurations wherein both reactants are in the LE or both in TE, and note that this analysis can be extended to cases wherein the reactants are placed in different buffers. To quantitatively capture the effect of initial sample placement, we define

$$\varepsilon \equiv \frac{N_{AB}^{TE}}{N_{AB}^{LE}} \tag{24}$$

where ε describes the ratio of product, AB, formation when both reactants are initially loaded into the TE (numerator) versus loading both into the LE (denominator). An important limiting condition for this ratio of production rates is observed for process times t, which are significantly larger than the maximum of τ^{LE} and τ^{TE}. This regime is associated with long times (or equivalently larger distances to detector), high k_{on}^{eff} values, and high initial species concentration. In this regime, the amount of AB grows linearly with time, so the problem is still unsteady but eq 24 simplifies to

$$\varepsilon \cong \phi_B \tag{25}$$

MODEL RESULTS AND DISCUSSION

We first presented a simple formulation for sample ion concentration in the ATE (cf. Figure 1b), the zone from which sample ions can directly focus into the ITP peak. We also presented the ratio of initial LE and TE concentrations, γ, a critical parameter when sample is mixed with TE. We used these factors and the concept of (nondimensional) separability to quantify the relative influx rates as a function of initial sample location. In Figure 2, we plot ratio of influx rate for samples

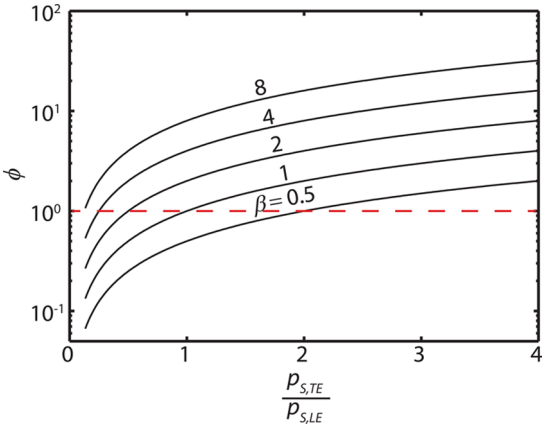

Figure 2. Ratio of influx rate from the TE and LE, ϕ, is plotted as a function of the ratio separabilites and β. ϕ linearly depends on the relative mobility of sample ions and surrounding buffer ions, and the adjustment in sample ion concentration upon entering the ATE zone from the TE. Unity (dashed red line) is a threshold value for ϕ. For $\phi > 1$, sample ions should be loaded in the TE. For $\phi < 1$, they should be loaded into the LE.

mixed with TE and LE, ϕ, as a ratio of the separabilities of sample in TE ($p_{s,TE}$) and sample in LE ($p_{s,LE}$), as per eq 11. ϕ is determined by the product of β and $p_{s,TE}/p_{s,LE}$. The proportionality to β shows the value of the field-amplified-type stacking of the sample as it migrates from TE to ATE. The magnitude of this stacking is achieved by establishing a high initial γ, and so leveraging the strict regulation of the ATE imposed by the LE. The proportionality to $p_{s,TE}/p_{s,LE}$ shows the relative importance of establishing a strong ratio of ion mobility to the *local* co-ion mobility. ϕ greater than unity implies superior influx rate by placing sample in the TE. Note that for fairly aggressive (but experimentally achievable) combinations of β and $p_{s,T}/p_{s,LE}$ (e.g., β = 0.25 and $p_{s,T}/p_{s,LE}$ = 0.25 or conversely β = 8 and $p_{s,T}/p_{s,LE} > 2$) there can be a 10-fold improvement in influx rate achieved by initially placing sample in LE vs TE (or vice versa for high β).

The influx rates of Figure 2 are very useful as initial design guidelines, but we note these are not exact criteria and that there may be other, practical considerations. For example, our eqs 11 and 12 neglect the effects of pH and ionic strength on electrophoretic mobility, and this may be particularly important for polyions.[31,35] In the Supporting Information, we derived influx rates accounting for influence of pH on electrophoretic mobility of singly ionized TE species. A further consideration is that the practical range of viable values of γ is constrained to different limits by Joule heating, maximum achievable voltage (e.g., to drive current through a low concentration TE), and the buffering capacity of the TE buffer (which can limit the maximum value of γ). The latter is important when using a separation channel volume that is not small relative to the volume of electrode reservoirs and low c_{TE} buffer in an electrode reservoir (see Persat et al.[36] for volume-specific estimates of buffering strength). See also Marshall[33] for a discussion of various ITP design parameters. Initial sample

DOI: 10.1021/acs.analchem.6b03467
Anal. Chem. XXXX, XXX, XXX−XXX

placement may also be driven by the need to have highly pure sample, as in some applications of peak-mode focusing of nucleic acids from complex samples.[7] The latter can drive a designer to lower values of $p_{s,TE}$ to ensure TE ions overspeed a relatively high mobility contaminant. However, in such cases, $p_{s,TE}$ may be significantly smaller than $p_{s,LE}$, prompting mixing sample with LE. For example, designing a TE buffer with pH close to that of the isoelectric point of a protein results in very low sample mobility in the TE, prompting placement of sample in the LE. On the other hand, users aiming to extract a wide range of analytes may choose high values of γ and $p_{s,TE}$ so placing the sample in TE would maximize influx. Type of contaminants is another important factor to consider, particularly in the presence of high-mobility, "LE-like" species such as chloride ions. In such cases, the sample may need to be diluted significantly in the TE or mixed with the LE.

Finally, we explored production rates (reaction rates) in ITP-aided reaction assays. We modified a model developed by Rubin et al.[20] The model used an effective association rate constant to account for nonideal sample distribution and its resulting impact on production rates. Figure 3a presents the

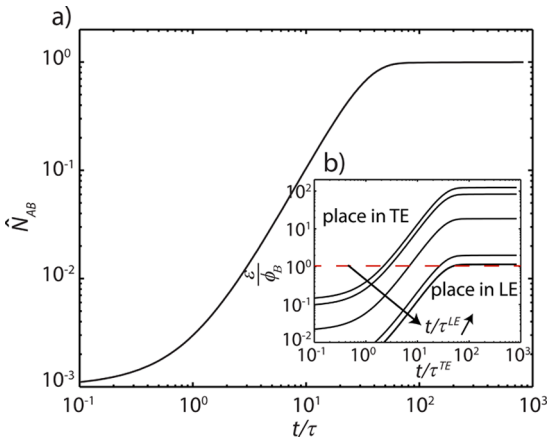

Figure 3. Production rates in ITP-aided assays. (a) Normalized amount of the reaction product, $\hat{N}_{AB}$, is plotted versus time normalized by characteristic ITP-driven reaction time, t/τ. For large times, the rate of product formation is equal to and limited by the influx rate of the limiting species, indicating a quasi-equilibrium (although unsteady) regime. (b) Inset shows dependence of product formation ratio ε (normalized by influx ratio parameter ϕ) on initial sample loading. We show the existence of regimes favoring loading in the LE (below the red dashed line) or TE (above the red dashed line). We find that for large values of both t/τ^{LE} and t/τ^{TE} (sufficient time of reaction), the production rate ratio ε is determined solely by influx rate ratio ϕ_B.

relationship between normalized product versus normalized time, as described by eq 19 and for limiting assumption eq 18. We normalized N_{AB} by the molar rate of limiting species (reactant B) entering the ITP zone, $Q_B t$, and time by the reaction time scale, τ, associated with the abundant species. At all times, the number of moles (and concentration) of species AB increases in time, and the problem is unsteady (even for long times). $\hat{N}_{AB}$ initially increases, reflecting the fact that the production rate of AB is increasing as reactants A and B enter the ITP zone and increase in concentration. The time scale of this initial period is governed by the dissociation and effective association rate constants (k_{off} and k_{on}^{eff}) and the (increasing) concentration of abundant species (reactant A). After times of about 50τ, $\hat{N}_{AB}$ reaches a plateau wherein the production rate of AB has grown until it reaches a constant value equal to and limited by the influx rate of the low abundance species. That is, ITP causes production rate to rise until it is constant and limited by the influx rate of the low-abundance species, establishing a quasi-equilibrium between production and influx. The limiting species enters the ITP zone and the (now fast) production rate quickly adjusts its concentration to the local equilibrium. Rubin's k_{on}^{eff} parameter (accounting for asymmetric peaks and imperfect overlap of peaks) directly modifies the time required to reach this equilibrium (e.g., prolonging the time for weakly overlapped species), but the process inevitably progresses toward this influx/production balance.

Figure 3b further shows how sample placement impacts the production rate in ITP-aided reaction assays. We normalized the ratio of product formed from TE and LE, ε, by the influx ratio ϕ_B. We find the existence of two regimes: a first where loading into LE is favorable over loading into TE (high values of t/τ^{LE} and low values of t/τ^{TE}), and a second where loading into TE is favorable (high values of t/τ^{TE} and low values of t/τ^{LE}). For large values of both t/τ^{TE} and t/τ^{LE}, the produced species ratio ε becomes equal to the influx ratio ϕ_B, a result we showed in eq 25. Again we see that, for sufficient normalized reaction times, the optimal production of species AB is achieved simply by maximizing the influx rate of the low abundance species.

SUMMARY

In summary, we presented an engineering analytical model examining influx and production rates in ITP. Influx rates are a strong function of initial sample placement and sample mobilities. ITP-aided production rates rise rapidly until they reach a constant value (linearly increasing product) limited by and equal to the influx rate of reactants. Our model identifies the key nondimensional parameters governing influx and production rates and enables a user to make informed decisions regarding optimal sample placement and ITP chemistry. In the Supporting Information, we present a case study of specifically nucleic acid extraction and reactions in ITP. The model provides intuition and design guidelines for ITP experiments.

ASSOCIATED CONTENT

Supporting Information

The Supporting Information is available free of charge on the ACS Publications website at DOI: 10.1021/acs.analchem.6b03467.

Derivation of effective mobilities and influx rates in ITP; fraction processed when sample is loaded in TE reservoir; case study: ITP-based DNA extraction and reaction assay design; fraction of sample loaded into TE reservoir that is processed by ITP; sample influx rates in DNA assays with ITP; and production rates in ITP-aided DNA hybridization assays (PDF)

AUTHOR INFORMATION

Corresponding Author

*Phone: 650-723-5689. Fax: 650-723-7657. E-mail: juan.santiago@stanford.edu.

Author Contributions

The manuscript was written through contributions of all authors. All authors have given approval to the final version of the manuscript.

DOI: 10.1021/acs.analchem.6b03467
Anal. Chem. XXXX, XXX, XXX−XXX

Notes

The authors declare no competing financial interest.

■ ACKNOWLEDGMENTS

The authors would like to acknowledge support from the National Science Foundation and the industrial members of the Center for Advanced Design and Manufacturing of Integrated Microfluidics (NSF I/UCRC Award Number IIP-1362165).

■ REFERENCES

(1) Everaerts, F. M.; Beckers, J. L.; Verheggen, T. P. E. M. *Isotachophoresis: Theory, Instrumentation, and Applications*; Elsevier Scientific Pub. Co.: Amsterdam, The Netherlands, 1976; p xiv, 418 pages.
(2) Bocek, P.; Deml, M.; Gebauer, P.; Dolnik, V. *Analytical Isotachophoresis*; VCH: Weinheim, Germany, 1988.
(3) Garcia-Schwarz, G.; Rogacs, A.; Bahga, S. S.; Santiago, J. G. *J. Visualized Exp.* **2012**, e3890.
(4) Persat, A.; Marshall, L. A.; Santiago, J. G. *Anal. Chem.* **2009**, *81*, 9507−11.
(5) Marshall, L. A.; Wu, L. L.; Babikian, S.; Bachman, M.; Santiago, J. G. *Anal. Chem.* **2012**, *84*, 9640−9645.
(6) Rogacs, A.; Qu, Y.; Santiago, J. G. *Anal. Chem.* **2012**, *84*, 5858−63.
(7) Rogacs, A.; Marshall, L. A.; Santiago, J. G. *J. Chromatogr A* **2014**, *1335*, 105−20.
(8) Kopwillem, A.; Merriman, W. G.; Cuddeback, R. M.; Smolka, A. J.; Bier, M. *J. Chromatogr.* **1976**, *118*, 35−46.
(9) Acevedo, F. *J. Chromatogr.* **1989**, *470*, 407−14.
(10) Qu, Y.; Marshall, L. A.; Santiago, J. G. *Anal. Chem.* **2014**, *86*, 7264−8.
(11) Eid, C.; Palko, J. W.; Katilius, E.; Santiago, J. G. *Anal. Chem.* **2015**, *87*, 6736−43.
(12) Sadecka, J.; Polonsky, J. *J. Chromatogr A* **1996**, *735*, 403−8.
(13) Bercovici, M.; Kaigala, G. V.; Mach, K. E.; Han, C. M.; Liao, J. C.; Santiago, J. G. *Anal. Chem.* **2011**, *83*, 4110−7.
(14) Borysiak, M. D.; Kimura, K. W.; Posner, J. D. *Lab Chip* **2015**, *15*, 1697−707.
(15) Bercovici, M.; Han, C. M.; Liao, J. C.; Santiago, J. G. *Proc. Natl. Acad. Sci. U. S. A.* **2012**, *109*, 11127−32.
(16) MacInnes, D. A.; Longsworth, L. G. *Chem. Rev.* **1932**, *11*, 171−230.
(17) Moore, G. T. *J. Chromatogr A* **1975**, *106*, 1−16.
(18) Khurana, T. K.; Santiago, J. G. *Anal. Chem.* **2008**, *80*, 6300−7.
(19) Garcia-Schwarz, G.; Bercovici, M.; Marshall, L. A.; Santiago, J. G. *J. Fluid Mech.* **2011**, *679*, 455−475.
(20) Rubin, S.; Schwartz, O.; Bercovici, M. *Phys. Fluids* **2014**, *26*, 012001.
(21) Saville, D. A.; Palusinski, O. A. *AIChE J.* **1986**, *32*, 207−214.
(22) Palusinski, O. A.; Graham, A.; Mosher, R. A.; Bier, M.; Saville, D. A. *AIChE J.* **1986**, *32*, 215−223.
(23) Eid, C.; Garcia-Schwarz, G.; Santiago, J. G. *Analyst* **2013**, *138*, 3117−20.
(24) Karsenty, M.; Rubin, S.; Bercovici, M. *Anal. Chem.* **2014**, *86*, 3028−36.
(25) Han, C. M.; Katilius, E.; Santiago, J. G. *Lab Chip* **2014**, *14*, 2958−67.
(26) Shkolnikov, V.; Santiago, J. G. *Anal. Chem.* **2014**, *86*, 6220−8.
(27) Persat, A.; Santiago, J. G. *Curr. Opin. Colloid Interface Sci.* **2016**, *24*, 52−63.
(28) Jovin, T. M. *Biochemistry* **1973**, *12*, 871−9.
(29) Alberty, R. A. *J. Am. Chem. Soc.* **1950**, *72*, 2361−2367.
(30) Everaerts, F. M.; Geurts, M.; Mikkers, F. E. P.; Verheggen, P. E. M. *J. Chromatogr.* **1976**, *119*, 129−155.
(31) Bahga, S. S.; Bercovici, M.; Santiago, J. G. *Electrophoresis* **2010**, *31*, 910−9.
(32) Bocek, P.; Gebauer, P.; Dolnik, V.; Foret, F. *J. Chromatogr.* **1985**, *334*, 157−95.
(33) Marshall, L. A. *Designing Automated Systems for Sample Preparation of Nucleic Acids Using Isotachophoresis*. Ph.D. Thesis, Stanford University, Stanford, CA, 2013.
(34) Persat, A.; Santiago, J. G. *Anal. Chem.* **2011**, *83*, 2310−6.
(35) Saifer, A.; Corey, H. *J. Biol. Chem.* **1955**, *217*, 23−30.
(36) Persat, A.; Suss, M. E.; Santiago, J. G. *Lab Chip* **2009**, *9*, 2454−69.

DOI: 10.1021/acs.analchem.6b03467
Anal. Chem. XXXX, XXX, XXX−XXX